Lithos 119 (2010) 137–146

Contents lists available at ScienceDirect

Lithos

journal homepage: www.elsevier.com/locate/lithos

Re–Os isotopic constraints on the genesis of the Limahe Ni–Cu deposit in the Emeishan large igneous province, SW China

Yan Tao [a,*], Chusi Li [b], Ruizhong Hu [a], Liang Qi [a], Wenjun Qu [c], Andao Du [c]

[a] State Key Laboratory of Ore Deposit Geochemistry, Institute of Geochemistry, Chinese Academy of Sciences, Guiyang, 550002, China
[b] Department of Geological Sciences, Indiana University, Bloomington, IN 47405, USA
[c] Chinese Academy of Geological Sciences, National Research Center for Geo-Analysis, Beijing, 100037, China

ARTICLE INFO

Article history:
Received 16 August 2009
Accepted 9 February 2010
Available online 19 Febuary 2010

Keywords:
Re–Os isotopes
Ni–Cu deposit
Ultramafic rocks
Limahe intrusion
Emeishan large igneous province

ABSTRACT

There are three types of magmatic sulfide deposits (sulfide-poor PGE deposit, sulfide-rich Ni–Cu deposit and Ni–Cu–PGE deposit) associated with mafic–ultramafic intrusions in the Late-Permian Emeishan large igneous province, SW China. The Limahe deposit represents a sulfide-rich Ni–Cu deposit in the region. Re–Os concentrations and isotopic compositions of the sulfide ores and associated ultramafic rocks in the Limahe intrusion are used to evaluate the relationships between magma evolution and oregenesis. There are two types of sulfide-barren olivine websterites in the Limahe intrusion: one is PGE depleted and the other is PGE undepleted. The PGE undepleted olivine websterites have $\gamma Os_{(260\,Ma)}$ between 5 and 8, whereas a PGE depleted olivine websterite sample has a $\gamma Os_{(260\,Ma)}$ value of ~30. A disseminated sulfide ore sample has a $\gamma Os_{(260\,Ma)}$ value close to 77. Net-textured sulfide ores and sulfide separates from net-textured sulfide ores have the highest $\gamma Os_{(260\,Ma)}$ values, varying between 102 and 124. The results can be explained by successive contamination of a mantle-derived magma with the lower and upper crusts during magma ascent. Mixing calculations indicate that the total amount of crustal contamination is ~15%. The concentrations of Os and Re–Os isotopes in the sulfide ores of the Limahe deposit are consistent with the sulfide liquids that segregated from a PGE depleted magma due to previous sulfide segregation. Higher $\gamma Os_{(260\,Ma)}$ values in the sulfide ores than the sulfide-barren ultramafic rocks in the Limahe intrusion suggest that crustal contamination played a critical role in sulfide saturation. Significant variations in Os concentrations and Re–Os isotopes in the Limahe intrusion suggest that multiple pulses of magma with variable crustal contamination were involved in the development of the intrusion. The different pulses of magma are likely related to each other by variable crustal contamination and sulfide segregation. Our new results support the hypothesis that the Limahe intrusion may represent a dynamic conduit through which magma successively ascended to higher crustal levels or to the surface.

1. Introduction

Magmatic Ni–Cu–PGE deposits associated with mafic–ultramafic intrusions have a wide variation in the composition of the bulk sulfide from PGE-rich to PGE-poor (Barnes et al., 1997; Li et al., 2001), and can be divided into three composition types (Naldrett, 2009): (1) sulfide-poor PGE deposit, the examples include the JM Reef of the Stillwater Complex in Montana, USA and the Merensky Reef of the Bushveld Complex, South Africa (Maier and Barnes, 2009); (2) Ni–Cu–PGE deposit, the examples include the Noril'sk-Talnakh Ni–Cu–PGE deposits, Siberia (Li et al., 2003, 2009; Lightfoot and Keays, 2005; Naldrett and Li, 2009) and the Jinchuan Ni–Cu deposit, western China (Song et al., 2009; Su et al., 2008; Tang et al., 2009); (3) sulfide-rich Ni–Cu deposit, of which the best example is the Voisey's Bay Ni–Cu–Co deposit in Labrador, Canada (Naldrett et al., 2009).

It is widely accepted that high metal contents in the bulk sulfide of PGE-rich deposits (including sulfide-poor PGE deposits and Ni–Cu–PGE deposits) may be due to the fact that the sulfide equilibrated with a large volume of magma, i.e., high *R* value (Barnes et al., 1997; Campbell and Naldrett, 1979). Several hypotheses have been advanced for sulfide-rich, PGE-poor Ni–Cu deposits: either these deposits formed at low *R* values close to *D* values for Ni and Cu but well below *D* values for PGEs (Campbell and Naldrett, 1979); or parent magmas formed at sufficiently low degrees of partial melting to leave sulfides and PGEs in the mantle (Arndt et al., 2005; Barnes and Lightfood, 2005); or magmas underwent a previous episode of sulfide segregation at depth, prior to the episode which formed the orebodies (Barnes, 2004; Lightfoot and Keays, 2005).

There are many magmatic Ni–Cu–PGE deposits in the Late-Permian (260 Ma) Emeishan large igneous province (ELIP), SW China, hosted by small mafic–ultramafic intrusions that are coeval with the Emeishan flood basalts and are considered to have genetic

* Corresponding author. Institute of Geochemistry, Chinese Academy of Sciences State Key Laboratory of Ore Deposit Geochemistry Guanshui road #46 Guiyang, Guizhou 550002 China. Tel.: +86 851 5891665; fax: +86 851 5891664.

0024-4937/$ – see front matter © 2010 Elsevier B.V. All rights reserved.
doi:10.1016/j.lithos.2010.02.006

relation with the hypothetical Emeishan mantle plume (Zhou et al., 2008). The sulfide deposits show a wide variation in the composition of the bulk sulfide and constitute a series of mineralization from PGE-rich to PGE-poor (Song et al., 2008). The three major types of magmatic Ni–Cu–PGE deposits associated with mafic–ultramafic intrusions in the world (Naldrett, 2009) have their equivalents in the ELIP: the Jinbaoshan deposit represents a sulfide-poor PGE deposit (Tao et al., 2007; Wang et al., 2005); the Yangliuping deposit represents a sulfide-rich Ni–Cu–PGE deposit (Song et al., 2003); and the Limahe and Baimazhai deposits are the best examples of sulfide-rich Ni–Cu deposits in the region (Sun et al., 2008; Tao et al., 2008; Wang et al., 2006, 2007). The coexistence of different types of magmatic sulfide deposits associated with a single event of continental basaltic magmatism in the Emeishan region provides an excellent opportunity to evaluate the relationships between regional basaltic magmatism and metallogeny. To this end we have carried out an integrated study of the Limahe deposit. The mineralogical, petrological, and S and Sm–Nd isotopic data have been reported in our previous paper (Tao et al., 2008). In this paper we report new Re–Os isotopic data that may provide additional constraints on the genesis of the deposit. The Re–Os isotope system is a sensitive tracer of magmatic evolution and ore-forming processes because of the strong fractionation of Re from Os between the crust and mantle, and the consequent sensitivity of Os isotopes to crustal contamination and because they offer a direct measurement of metals involved in magmatic ore genesis (Lambert et al., 1999; Ripley et al., 1999; Ripley et al., 2008, Shirey, 1997).

2. Geological background

In the western part of the Yangtze block, there are large volumes of flood basalts which erupted during the Late-Permian (Fig. 1). The flood basalts constitute a major part of the ELIP. They cover over an area of 5×10^5 km^2, with thickness ranging from several hundred meters up to 5 km (Chung and Jahn, 1995; Fan et al., 2008; Song et al., 2001; Xiao et al., 2004; Xu et al, 2001; Zhang et al., 2008a; Zhou et al, 2006). The ELIP is considered to be a good example of mantle plume magmatism in continental setting by many researchers (Ali et al.,

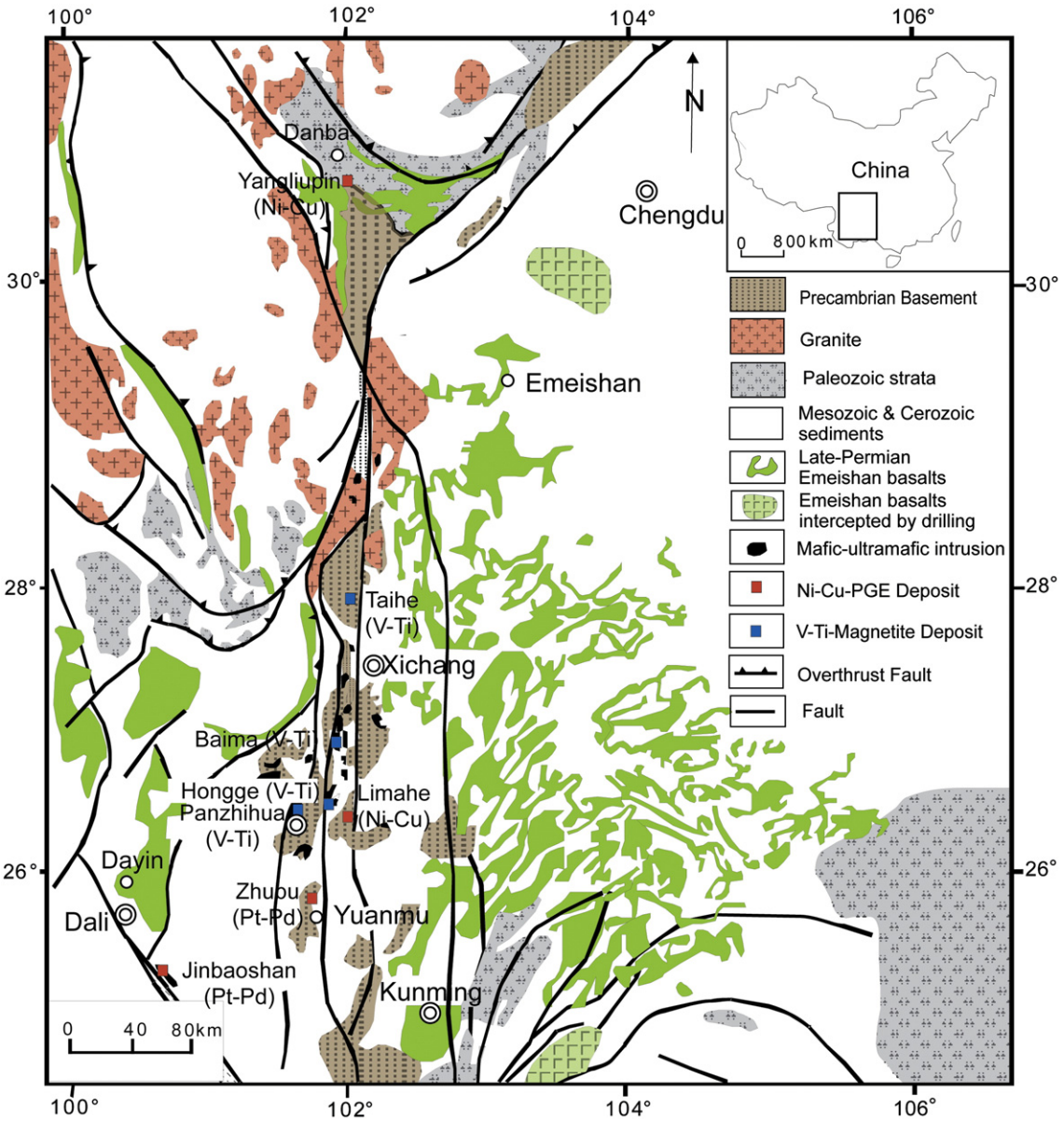

Fig. 1. Distribution of the Emeishan continental flood basalts and some coeval mafic–ultramafic intrusions that host different types of magmatic ore deposits. Modified from Wang et al. (2005).

2005; He et al., 2003; Shellnutt et al., 2009a; Xu et al., 2004, 2008; Zhou et al, 2002).

Mafic–ultramafic intrusions and coeval felsic intrusions are exposed mostly in the central part of the ELIP. The SHRIMP zircon U–Pb ages indicate that the crystallization of the intrusive rocks are contemporaneous with the eruption of the flood basalts in the region (Shellnutt and Zhou, 2007; Tao et al., 2009, Zhong and Zhu, 2006; Zhong et al., 2007; Zhou et al. 2008). Some relatively large, mafic intrusions of the ELIP host world-class Fe–Ti–V oxide deposits (e.g., Pang et al., 2008, 2009; Shellnutt et al., 2009b; Zhong et al., 2004; Zhou et al., 2005) while some relatively small, mafic–ultramafic intrusions host magmatic sulfide deposits (e.g., Ma et al., 2009; Song, et al., 2003; Tao et al., 2007, 2008; Wang et al., 2006). As shown in Fig. 1, both types of deposits have been found mostly in the central part of the ELIP where uplift and erosion are most significant.

The geology, mineral chemistry, whole rock elemental and Sr–Nd isotopic geochemistry of the Limahe deposit have been given previously by Tao et al. (2008) and Zhang et al. (2009). The surface exposure of the Limahe intrusion is about 900 m long and 180 m wide (Fig. 2a). The vertical downward extension of the intrusion exceeds 200 m. Fig. 2b illustrates the internal structure of the Limahe intrusion and associated sulfide mineralization. Immediate country rocks to the intrusion are Proterozoic pyrite-bearing quartzites, graphitic slates and siliceous limestones. The intrusion is divided to two lithologic units: a mafic unit to the east and an ultramafic unit to the west. The mafic unit comprises a diorite zone at the top and a gabbro zone at the bottom. The ultramafic unit, which constitutes about a third of the total volume of the intrusion, comprises wehrlite and olivine websterite with gradational contact between them. It extends to greater depths than the mafic unit. In many places the ultramafic unit has fault contacts with country rocks.

Sulfide mineralization, in the forms of disseminated, net-textured and massive sulfides (pyrrhotite, pentlandite and chalcopyrite) (Fig. 3b, c and d), is restricted to the ultramafic unit. Several massive sulfide lenses occur along the contacts with sedimentary country rocks. The overall orientations of massive and net-textured sulfide zones are sub-parallel to layering in the mafic unit, suggesting that the west contact was originally the base of the intrusion.

The ultramafic unit is an olivine-cumulate rock characterized by abundant olivine inclusions enclosed by poikilitic augite (Fig. 3a) and high MgO contents between 23 and 38 wt.%. The mafic unit has much lower MgO contents, varying between 5 and 13 wt.%. There is a large gap between the contents of MgO in these two rock units due to different cumulus mineralogy (i.e., olivine versus clinopyroxene). Some diorite samples have low SiO_2, and high TiO_2 and FeO contents due to abundant cumulus Fe–Ti oxides. The trace element patterns of the Limahe intrusion (Tao et al., 2008) and the Emeishan picrites (Zhang et al., 2006) are similar. The Limahe intrusive rocks are characterized by negative Nb anomalies that have been attributed to crustal contamination (Tao et al., 2008).

Olivine in the ultramafic unit of the Limahe intrusion has Fo contents between 79 and 86 mol% and Ni contents between 1300 and

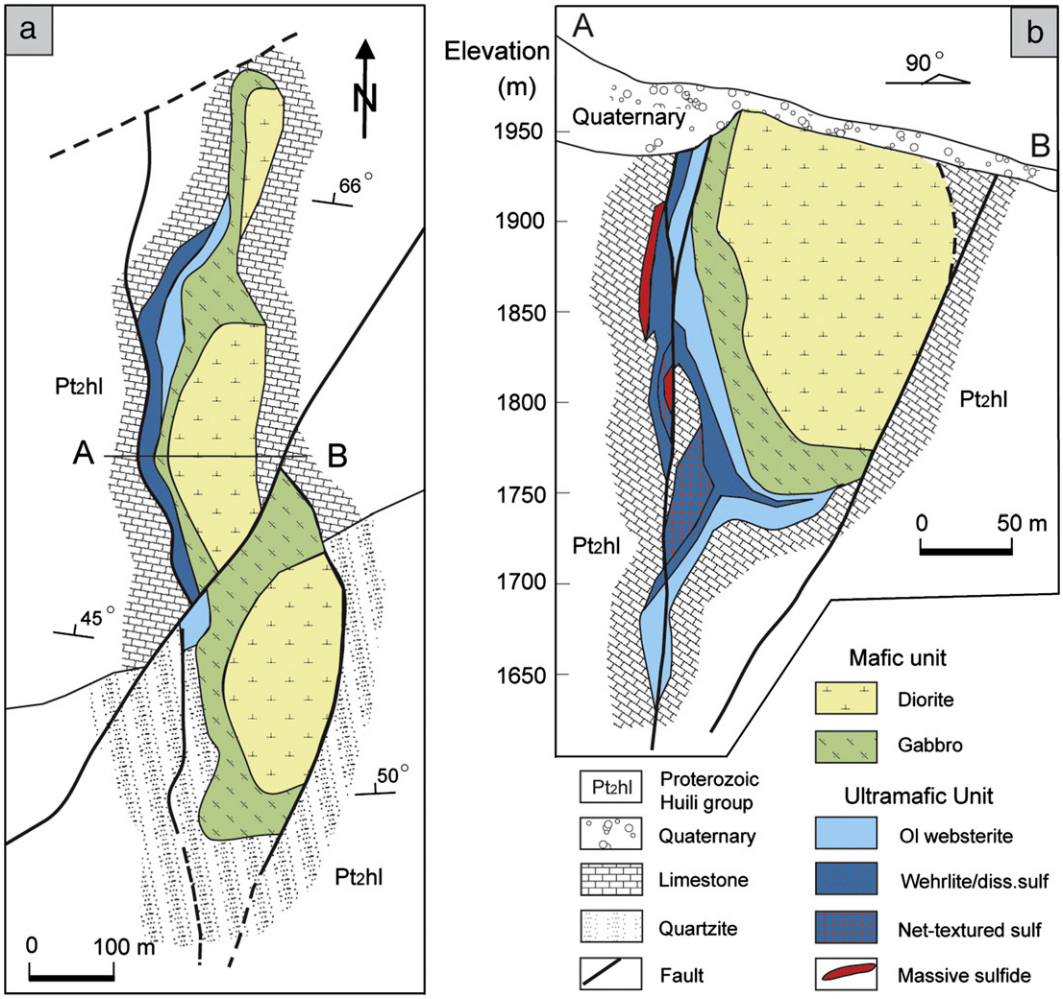

Fig. 2. Plan view (a) and cross-section (b) of the Limahe mafic–ultramafic intrusion.
After Tao et al. (2008).

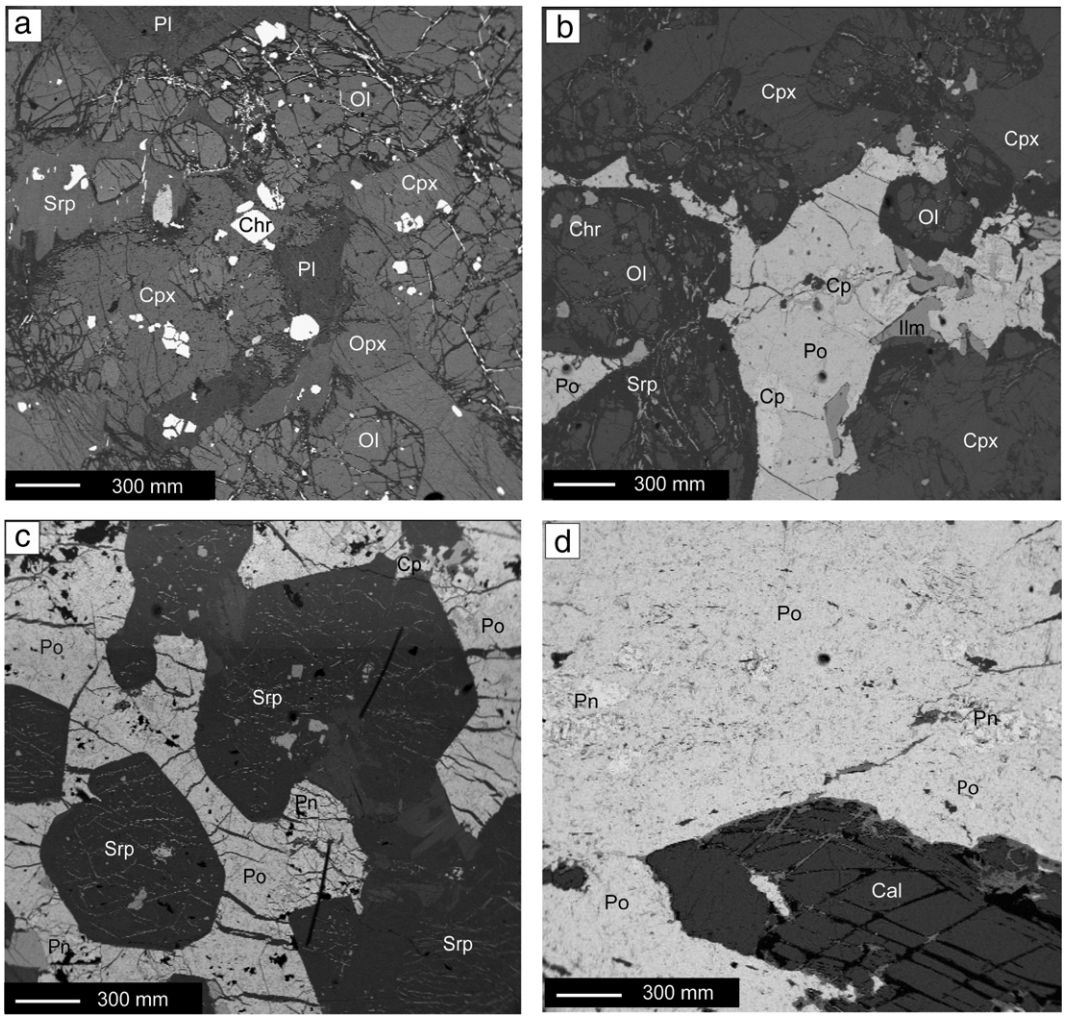

Fig. 3. Back scattered electron images. (a) Sulfide-barren olivine websterite. (b) Disseminated sulfide ore. (c) Net-textured sulfide ore. (d) Massive sulfide ore. Ol — olivine, Cpx — clinopyroxene, Pl — plagioclase, Chr — chromite, Srp — serpentine, ilm — ilmenite, Cp — chalcopyrite, Po — pyrrhotite, Pn — pentlandite, Cal — calcite.

2000 ppm. These values are slightly lower than the Fo and Ni contents of olivine phenocrysts in the Emeishan picrites (Zhang et al., 2006), suggesting that the parental magma of the Limahe intrusion is more fractionated than the Emeishan picrites.

3. Samples and analytical methods

The samples used in this study include sulfide-barren olivine websterite (Fig. 3a), disseminated sulfide ore (Fig. 3b), net-textured sulfide ore (Fig. 3c), massive sulfide ore (Fig. 3d) and sulfide mineral separates from net-textured sulfide ore samples. Sample LMS4 is a disseminated sulfide ore containing ~4 vol.% total sulfides. Samples LMK6, LMK9, LMK7 and LMK3 are net-textured sulfide ores containing 30–70 vol.% total sulfides. The sulfide mineral separates were separated from the net-textured sulfide ore samples by floatation. Sample LMU3 is a sulfide-barren olivine websterite with low PGE contents (1.7 ppb Pt, 0.8 ppb Pd: Tao et al., 2008). Samples LMU4 and LMU5 are sulfide-barren olivine websterites with higher PGE contents (~7 ppb Pt, ~5 ppb Pd: Tao et al., 2008). The sample with low PGE contents (LMU3) is referred to as PGE depleted and the samples (LMU4 and LMU5) with higher PGE contents are referred to as PGE undepleted thereafter. Both PGE depleted and undepleted olivine websterites do not contain visible sulfides and have similar silicate mineral modal compositions. They contain 15–40 vol.% olivine, 30–50 vol.% clinopyroxene, 15–30 vol.% plagioclase, 10–20 vol.% orthopyroxene, and minor hornblende, phlogopite, ilmenite and chromite (Fig. 3a). Olivine crystals in the samples are partly altered to serpentine plus fine-grained magnetite. Disseminated and net-textured sulfide ore samples comprise, in the order of decreasing abundance, pyrrhotite, pentlandite and chalcopyrite. The massive sulfide samples used in this study are dominated by pyrrhotite and contain calcite inclusions (Fig. 3d).

The Re–Os isotope analyses were carried out in the Re–Os laboratory of the National Research Center of Geo-Analysis, Chinese Academy of Geosciences, Beijing. Re–Os isotopic data were obtained by isotope dilution HR-ICP-MS methods (ELEMENT II). We used a Carius tube (a thick-wall borosilicate glass ampoule) to digest the samples. The weighed sample was loaded in a Carius tube through a thin neck long funnel. The ^{190}Os and ^{185}Re spike solutions from the Oak Ridge National Laboratory, USA, 2 mL of 12 M HCl and 6 mL of 15 M HNO_3 were loaded to the bottom of the tube at −50 to −80 °C. The top of the tube was sealed using an oxygen-propane torch. The tube was then placed in a stainless-steel jacket and heated for 10 h at 230 °C. Upon cooling, the bottom part of tube was kept frozen while the tube was broken at its neck. The contents of the tube were poured into a distillation flask and the residue was washed out of the tube with 40 mL pure water.

Os was distilled two times. During the first time, OsO_4 was distilled at 105–110 °C for 50 min and was collected in 10 mL pure water. The residual Re-bearing solution was saved in a 50 mL beaker for Re

separation. The water trap solution plus 40 mL water were distilled a second time. The OsO_4 was distilled for 1 h and collected in 10 mL water for Os isotopic analysis by ICP-MS (TJA PQ-EXCELL).

The Re-bearing solution was evaporated to dryness. One mL pure water was then added, and the solution was heated twice to dryness. Ten mL 20% NaOH was added to the residue, and the Re was extracted using 10 mL acetone in a 120 mL Teflon separation funnel. Two mL of 20% NaOH was added to the Re and transferred to a 100 mL beaker in which 2 mL water was present. The Re solution was evaporated to dryness, and dissolved with 2% HNO_3 to form a final solution for Re isotopic analysis by HR-ICP-MS.

4. Result

The Re–Os concentrations in whole rocks and the Re–Os isotopic compositions of the Limahe samples are listed in Table 1. The initial Os isotopic ratio $^{187}Os/^{188}Os$ and γOs_I are calculated based on a crystallization age of 260 Ma for the Limahe intrusion given by Zhou et al. (2008).

Two of the three massive sulfide samples analyzed have lower Os concentrations and higher $\gamma Os_{(260\,Ma)}$ than the disseminated and net-textured sulfide ore samples. The $\gamma Os_{(260\,Ma)}$ values of the massive sulfide samples vary between ~700 and ~800, close to crustal values. The presence of calcite inclusions in the massive sulfide samples (Fig. 3d) suggests possible overprinting of post-magmatic hydrothermal alteration in the samples. Therefore, we will exclude the results of the massive sulfide samples from the following discussion.

The Re and Os concentrations in the sulfide-barren olivine websterites of the Limahe intrusion are similar to the values in the coeval picrites and the ultramafic rocks of the Jinbaoshan intrusion (Fig. 4). The PGE undepleted olivine websterites of the Limahe intrusion contain ~0.9 ppb Re and 1.8 ppb Os, and have Re/Os ratios close to 0.5. These values are similar to that of komatiites (Fig. 5). The sulfide-bearing samples of the Limahe and Jinbaoshan intrusions are different in Re and Os concentrations. The Limahe sulfide-bearing samples are relatively high in Re whereas the Jinbaoshan sulfide-bearing samples are high in Os (Fig. 4). A clear positive correlation between Re and Os exists in the Jinbaoshan sulfide-bearing samples but not in the Limahe sulfide-bearing samples. As shown in Fig. 5, the Os concentrations and Re/Os ratios of the sulfide-bearing samples from the Limahe deposit are different from those from the Jinbaoshan deposit but similar to those from the Voisey's Bay and Duluth Ni–Cu deposits.

Excluding the massive sulfide samples, the sulfide-rich (>20 wt.% S) samples of the Limahe deposit yield an isochron age of 265 ± 35 Ma and an initial $^{187}Os/^{188}Os_{(260\,Ma)}$ of 0.254 corresponding to a $\gamma Os_{(260\,Ma)}$ of 102 (Fig. 6a). The Re–Os isochron age is similar to the more precise SHRIMP zircon U–Pb age of 263 ± 3 Ma given by Zhou et al. (2008). The sulfide-poor samples (<2 wt.% S) from the Limahe deposit plot below the 265 ± 35 Ma isochron (Fig. 6a) and have lower calculated $\gamma Os_{(260\,Ma)}$ values (Fig. 6b). The $\gamma Os_{(260\,Ma)}$ values decrease with $^{187}Re/^{188}Os$ ratios in the sulfide-poor and sulfide-barren samples from the Limahe intrusion (Fig. 6b). Such correlation does not exist in the sulfide-bearing samples.

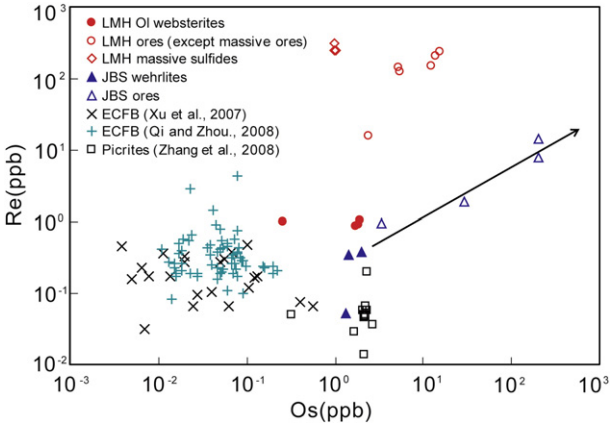

Fig. 4. Plot of Re versus Os contents in the samples from the Limahe deposit. Data for the Jinbaoshan deposit are from Tao et al. (2007). Data for the Emieshan continental flood basalts (ECFB) are from Xu et al. (2007) and Qi and Zhou (2008). Data for the ELIP picrites are from Zhang et al. (2008b).

The sulfide-barren, PGE undepleted olivine websterites of the Limahe intrusion have $\gamma Os_{(260\,Ma)}$ between ~5 and ~8, similar to the values of mantle plume-derived melts (c.f., Horan et al., 1995; Shirey, 1997). The sulfide-barren, PGE depleted olivine websterite has a $\gamma Os_{(260\,Ma)}$ value of ~30. The sulfide-rich samples and their sulfide mineral separates have higher $\gamma Os_{(260\,Ma)}$ values, varying between ~102 and ~124. The sulfide-poor sample has a moderate $\gamma Os_{(260\,Ma)}$ of ~77. The calculated $\gamma Os_{(t=260\,Ma)}$ values of the Limahe samples increase logarithmically with S contents in the samples (Fig. 7).

5. Discussion

5.1. Physical mixing

Our results suggest that the sulfide and silicate portions of the Limahe intrusion may have different Os isotopic compositions. The sulfide-bearing samples of the intrusion can be explained by mixing of a sulfide liquid containing relatively high radiogenic Os with silicate cumulates containing much lower radiogenic Os. This is illustrated in Fig. 8. Due to much higher Os concentration in the sulfide liquid than

Table 1
Results of Re–Os isotopic analyses of the Limahe Ni–Cu deposit in the ELIP (d), duplicate analysis; SS, sulfide separate; nd, not determined. Uncertainties of Re–Os isotope compositions are reported for 1δ standard errors. $\gamma Os = 100[(^{187}Os/^{188}Os)_{initial}/(^{187}Os/^{188}Os)_{CHUR} - 1]$, where $^{187}Os/^{188}Os$ (CHUR) at 260 Ma = 0.125846. A present-day $(^{187}Re/^{188}Os)^{now}_{CHUR} = 0.3972$, $(^{187}Os/^{188}Os)^{now}_{CHUR} = 0.12757$ (Walker and Morgan, 1989), a decay constant $\lambda^{187}_{Re} = 1.666 \times 10^{-11}$ year^{-1} (Smoliar et al., 1996) were used in the calculations.

Sample	Description	S	Re	Os	$^{187}Re/^{188}Os$	1σ	$^{187}Os/^{188}Os$	1σ	$^{187}Os/^{188}Os$	γOs
		wt.%	ppb	ppb					260 Ma	260 Ma
LMU3	Olivine websterite	0.14	1.007	0.2614	18.43	0.61	0.24	0.02	0.16	30.0
LMU4	Olivine websterite	0.20	0.86	1.730	2.367	0.080	0.14	0	0.13	4.9
LMU4(d)	Olivine websterite	nd	0.9	1.838	2.332	0.066	0.14	0.01	0.1340	6.5
LMU5	Olivine websterite	0.18	1.049	1.938	2.589	0.069	0.15	0	0.14	7.7
LMS4	Disseminated ore	1.76	15.87	2.392	31.73	1.34	0.36	0	0.22	76.7
LMK6	Net-textured ore	21.79	149.4	12.47	57.28	0.81	0.52	0.01	0.27	111.9
LMK3	Net-textured ore	28.33	147.2	5.165	136.3	1.4	0.87	0.02	0.28	123.9
LMK7s	SS (net-textured ore)	nd	127.7	5.475	112.1	1.7	0.74	0.01	0.25	101.7
LMK9-1 s	SS (net-textured ore)	nd	239.3	15.63	73.61	1.10	0.58	0.02	0.2590	105.8
LMK9-2 s	SS (net-textured ore)	nd	205.7	13.88	71.27	0.97	0.56	0.01	0.25	102.4
LMK2	Massive sulfide	35.43	311.2	0.9859	1510	22	7.54	0.04	0.99	687.3
LMK1	Massive sulfide	34.17	253.2	1.008	1208	17	6.33	0.0960	1.12	787.5
LMK1(d)	Massive sulfide	nd	255.3	0.9701	1258	23	6.5700	0.01	1.11	779.2

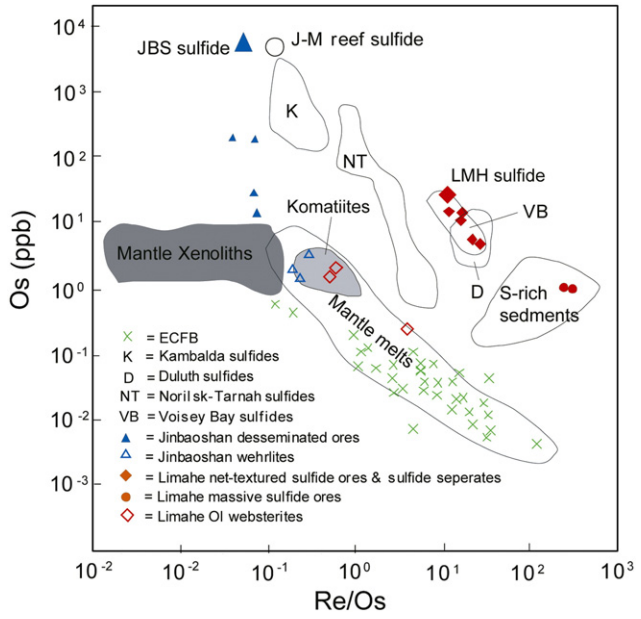

Fig. 5. Plot of Os content versus Re/Os for the Limahe deposit. Data for the Jinbaoshan deposit are from Tao et al. (2007). Data for the Emieshan continental flood basalts (ECFB) are from Xu et al. (2007) and Qi and Zhou (2008). Other data are from Lambert et al. (1999).

the silicate cumulates, the Os isotopic compositions in the mixtures are sensitive to change in sulfide content when the total contribution of sulfide liquid is below 30 wt.% but become much less sensitive to

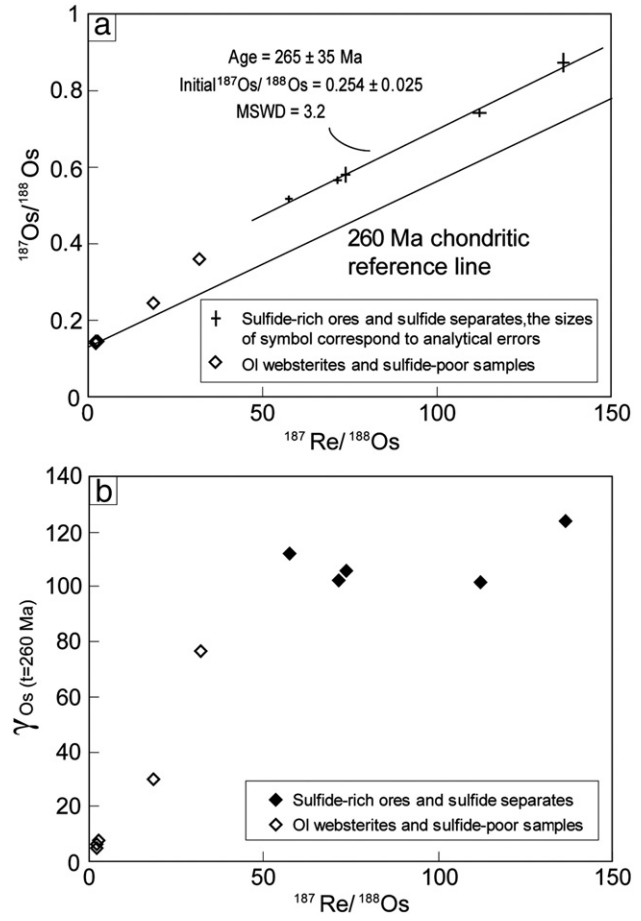

Fig. 6. Plots of Re–Os isotope compositions for the Limahe deposit and associated sulfide-barren rocks.

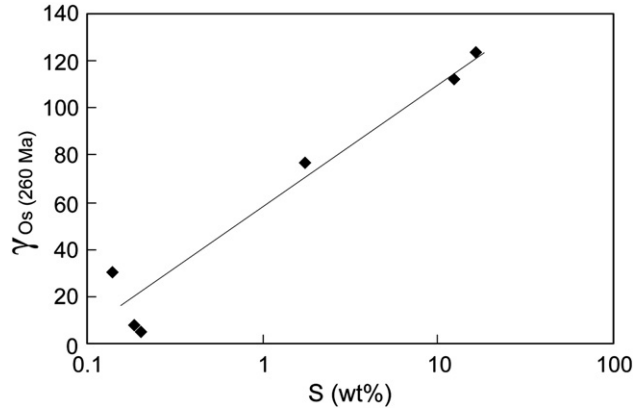

Fig. 7. Plot of $\gamma Os_{(260Ma)}$ versus logarithmic S contents in the Limahe samples.

such change when the total contribution of sulfide liquid exceeds 30 wt.%. The above physical mixing process may take place owning to a lower liquidus temperature for a sulfide liquid than a mafic magma. The different crystallization temperatures between them may allow a sulfide liquid to infiltrate a partially solidified cumulate in the intrusion. Alternatively, the variable Os isotopic compositions in the Limahe intrusion may be related to multiple pulses of magma with different degrees of crustal contamination. This will be further evaluated below.

5.2. Mass balance

The concentrations of Re and Os in the magmas of the Limahe intrusion may be estimated using the sulfide-barren websterite samples. The PGE undepleted websterite contains 0.9 ppb Re and 1.8 ppb Os. The Re/Os ratio of this sample is ~0.5. The PGE depleted websterite contains 1 ppb Re and 0.3 ppb Os. The Re/Os ratio of this sample is ~4. Based on their texture and mineral modal compositions, both samples may be interpreted to represent mixtures of 40% cumulus olivine plus 60% "trapped liquid". Assuming that olivine–melt $D^{Os}=3$ and $D^{Re}=0$, the concentrations of Re and Os in the "trapped liquid" portion of the PGE undepleted websterite sample are estimated to be 1.5 ppb and 1 ppb, respectively; the concentrations of Re and Os in the "trapped liquid" portion of the PGE depleted websterite sample are estimated to be 1.7 ppb, and 0.14 ppb,

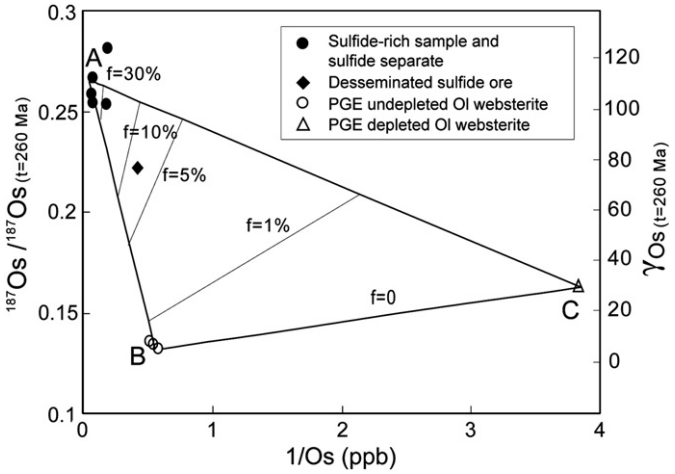

Fig. 8. Physical mixing model for the Limahe deposit. f = fraction of sulfide in the mixtures, A = a sulfide liquid containing 22 ppb Os with $^{187}Os/^{188}Os_{(260\ Ma)}=0.2667$, B = a PGE undepleted olivine websterite containing 1.838 ppb Os with $^{187}Os/^{188}Os_{(260\ Ma)}=0.1340$, C = a PGE depleted olivine websterite containing 0.2614 ppb Os with $^{187}Os/^{188}Os_{(260\ Ma)}=0.1636$.

respectively. Selective depletion of IPGE (Os, Ir and Ru) that may be related to significant alloy segregation at depth has been found in some Emeishan basalts (Qi and Zhou, 2008). However, the Limahe PGE depleted websterite samples are depleted in all PGE (Tao et al., 2008), not just IPGE alone. Another line of evidence that the parental magma of the Limahe deposit did not experience significant segregation of IPGE-bearing alloys at depth is the lack of IPGE depletion relative to other PGE in the sulfide ores (Tao et al., 2008). This is also true for the coeval Jinbaoshan Pt–Pd deposit (Tao et al., 2007). Therefore, we believe that PGE depletion in some of the sulfide-barren websterite samples from the Limahe intrusion is related to sulfide segregation instead of alloy segregation at depth, and that the different metal tenors (i.e., concentrations in recalculated 100% sulfide) in the Limahe and Jinbaoshan deposits are due to different R factors as well as different parental magma compositions.

Fig. 9 illustrates the results of our numerical modeling based on the concept of multiple sulfide segregations. The contents of Re and Os in the primary magma estimated from the PGE undepleted websterite samples from the Limahe and Jinbaoshan deposits are similar. The estimated Os contents in the primary magma for these intrusions are higher than in the coeval basalts (Qi and Zhou, 2008; Xu et al., 2007) but within the range of the coeval picrites (Hanski et al., 2004; Zhang et al., 2008b). In our calculations we used the mass balance equation of Campbell and Naldrett (1979) and sulfide/magma $D^{Os} = 30{,}000$ and $D^{Re} = 500$. The D values used in our calculations are within the ranges of experiments by Fleet et al. (1999), Brenan (2008) and Righter et al. (2004). As shown in Fig. 9, the bulk sulfide ores (recalculated to 100% sulfide) of the Jinbaoshan deposit are consistent with the sulfide liquids segregated at $R>10{,}000$ from the primary magma. However, the bulk sulfide ores of the Limahe deposit contain Os that is too low to be produced by the primary magma. They are more consistent with the products of a daughter magma derived from the primary magma by previous sulfide segregation at depth.

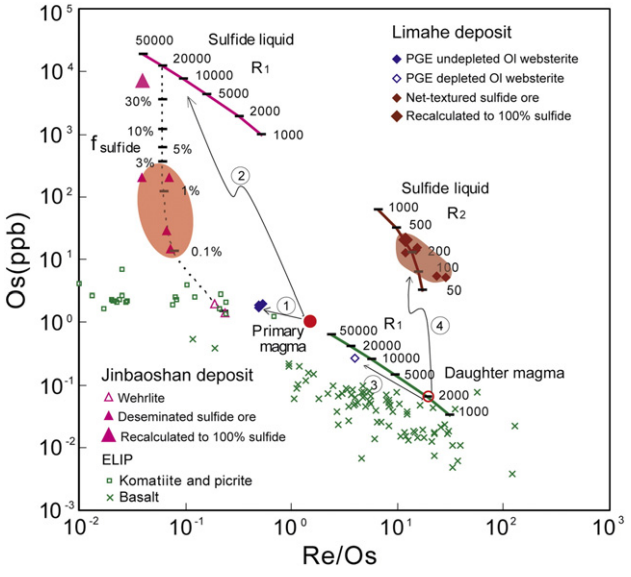

Fig. 9. Modeling of sulfide segregation at Jinbaoshan and Limahe based on Os contents and Re/Os ratios. The compositions of the assumed primary magma are estimated from the PGE undepleted ultramafic rocks from the Limahe and Jinbaoshan intrusions. The daughter magma is a derivative of the primary magma after sulfide segregation at depth. In our calculations we used sulfide–magma D^{Os} of 30,000 and D^{Re} of 500. The $f_{sulfide}$ values represent the proportions of sulfide liquid in samples formed by mixing of sulfide liquid with coexisting silicate melt. ① Dilution due to accumulation of olivine crystallized from the primary magma; ② sulfide liquids segregated from the primary magma at variable R factors (R_1); ③ dilution due to accumulation of olivine crystallized from the daughter magma; ④ sulfide liquids segregated from the daughter magma at variable R factors (R_2). Data for the picrites of the ELIP are from Zhang et al. (2008b) and Hanski et al. (2004). Data for the basalts of the ELIP are from Xu et al. (2007) and Qi and Zhou (2008). Data for the Jinbaoshan deposit are from Tao et al. (2007).

The results of numerical modeling based on Os and Re contents are supported by the results of numerical modeling based on Cu and Pd contents. This is illustrated in Fig. 10. The content of Pd and Cu/Pd ratio in the primary magma estimated from the sulfide-barren ultramafic rocks in the Jinbaoshan and Limahe intrusions are within the ranges of the coeval volcanic rocks in the ELIP (Qi and Zhou, 2008; Zhang et al., 2008b; Zhong and Zhu, 2006). The sulfide mineralized samples of the Jinbaoshan intrusion represent variable amounts of sulfide liquids segregated at $R>10000$ from the primary magma. The sulfide mineralized samples of the Limahe intrusion represent variable amounts of sulfide liquids segregated at $R>300$ from the daughter magma that had experienced previous sulfide segregation from the primary magma. In our calculations we used the sulfide–magma D^{Cu} of 1400 and D^{Pd} of 30,000 from Peach and Mathez (1996).

5.3. Crustal contamination

High γOs values of the Limahe sulfide ores (up to 120) are consistent with significant contamination of the parental magma with crustal materials. Using Nd–Sr isotopes of the associated intrusive rocks, Tao et al. (2008) estimated 10–15% crustal contamination for the Limahe intrusion. Fig. 11 illustrates the results of our new calculations using both Nd and Os isotopes. Data for the Jinbaoshan deposit are included in the figure for a comparison. The γOs and $\varepsilon Nd_{(t=260\,Ma)}$ values of the Jinbaoshan deposit are within the range of the coeval Emeishan basalts. Three samples from the Limahe deposit fall within the field of the Emeishan basalts. Another three samples from the Limahe deposit have higher γOs values and are displaced to the right. With the exception of one sample, all other samples from the Limahe deposit fall between the two mixing lines between a hypothetical mantle plume-derived magma coded as "picrite" and the lower crust and upper crust-1, suggesting that the Limahe magma may have experienced contamination with both the lower and upper crusts during magma ascent. Based on this result, we have proposed a 2-stage contamination model to explain the Re–Os isotopic variations in the Limahe intrusion. The parameters and procedures used in our calculations are summarized in Table 2 and the results are illustrated in Fig. 12. Our calculations indicate that the two-stage contamination model can adequately explain the Re–Os isotopic compositions of the sulfide ores in the Limahe deposit if sulfide segregation took place in both stages. Immiscible sulfide liquids segregated during the first and second stages would have γOs values of ~30 and ~110, respectively. The former is similar to the values of the PGE depleted websterites

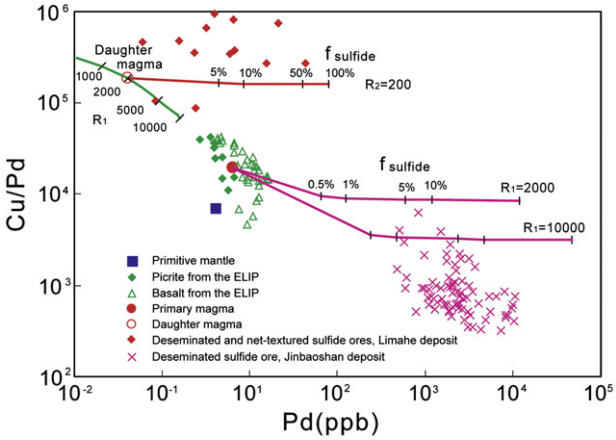

Fig. 10. Modeling of sulfide segregation based on Pd contents and Cu/Pd ratios. Data for the picrites of the ELIP are from Zhang et al. (2005). Data for the basalts of the ELIP are from Zhong et al. (2006) and Qi and Zhou (2008). Data for the Jinbaoshan deposit are from Tao et al. (2007) and an internal company report.

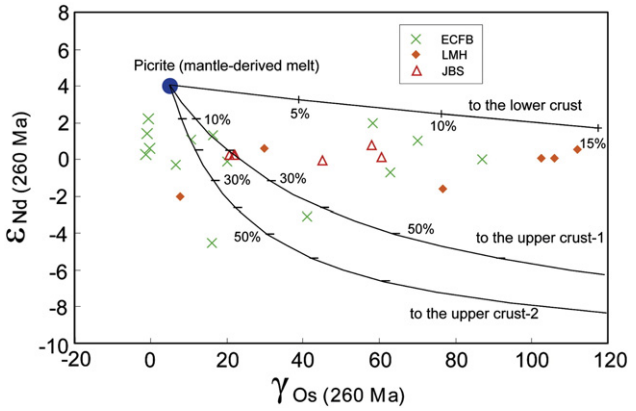

Fig. 11. Modeling of crustal contamination using γOs and εNd values. The εNd values of the Limahe intrusion (LMH) are from Tao et al. (2008). Data for the Emeishan continental flood basalts (ECFB) are from Xu et al. (2007). Data for the Jinbaoshan deposit (JBS) are from Tao et al. (2007). The "picrite" represents a hypothetical mantle plume-derived melt with Re–Os concentrations and isotopic compositions similar to that proposed by Arndt et al. (2003). The compositions of the end members used in our mixing calculations are from Esser and Turekian (1993), Saal et al. (1998), Ripley et al. (1999) and Lambert et al. (1999): picrite (mantle-derived melt), 1 ppb Os, γOs = 5, 20 ppm Nd, εNd = +4; Lower crust, 0.1 ppb Os, γOs = +6500, 11 ppm Nd, εNd = −22; upper crust-1, 0.05 ppb Os, γOs = +1250, 32 ppm Nd, εNd = −10; Upper crust-2, 0.05 ppb Os, γOs = +540, 32 ppm Nd, εNd = −10.

and the latter is similar to the values of the bulk sulfide ores of the Limahe deposit.

5.4. Multiple pulses of magma

Our data suggest that at least 3 pulses of magma with different degrees of crustal contamination were involved in the development of the ultramafic unit of the Limahe intrusion: (1) a parental magma for the PGE undepleted websterites with $\gamma Os_{(260\,Ma)}$ of 5–8; (2) a parental magma for the PGE depleted websterites with $\gamma Os_{(260\,Ma)}$ of ~33, and (3) a parental magma for the net-textured sulfide ores with $\gamma Os_{(260\,Ma)}$ of >00. These 3 pulses of magma may be related to each other by variable crustal contamination at depth. As shown in Fig. 8, the disseminated sulfide ores of the Limahe deposit may have formed by infiltration of sulfide liquids in partially solidified olivine cumulates.

Table 2
Parameters and calculation procedures for a 2-stage contamination-sulfide segregation model for the Limahe deposit D^{Os} (sulfide/magma) = 30,000, D^{Re} (sulfide/magma) = 500 were used in our calculations. The compositions of the lower and upper crusts are from Esser and Turekian (1993), Saal et al. (1998) and Ripley et al. (1999). The PGE undepleted magma estimated from the composition of the sulfide-barren, PGE undepleted websterite of the Limahe intrusion was used as primary magma in our calculations.

		Re (ppb)	Os (ppb)	γOs	Re/Os
Lower crust		0.2	0.1	6500	2
Upper crust		0.4	0.05	1250	8
Uncontaminated magma		1.5	1	5	1.5
1st stage in lower crust	PGE undepleted magma with 7% contamination	1.41	0.93	29	1.51
	Sulfide liquid segregated at an *R* factor of 2000	564	1751	29	0.32
	Resultant PGE depleted magma	1.13	0.06	29	19.3
2nd stage in upper crust	PGE depleted magma with 7.6% contamination	1.07	0.06	110	18.7
	Sulfide liquid segregated at an *R* factor of 300	202	17	110	11.8
Bulk sulfide ore of the Limahe deposit		249	21	112	12

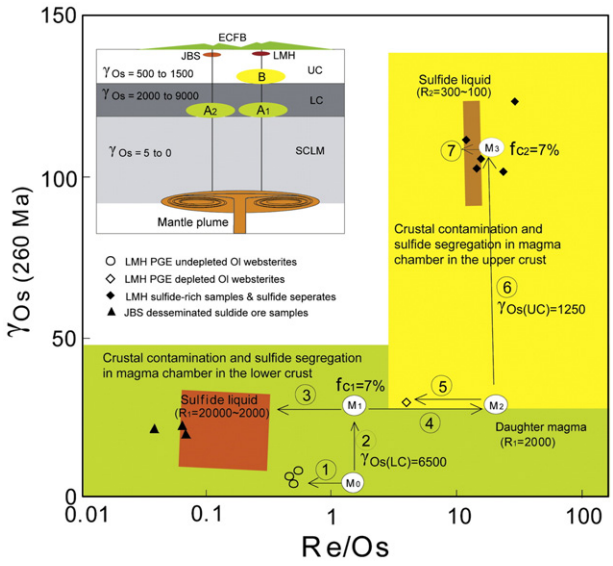

Fig. 12. A genetic model for the Limahe deposit based on $\gamma Os_{t=260\,Ma}$ and Re/Os. The compositions of disseminated sulfide ores from the Jinbaoshan deposit (Tao et al., 2007) are used for comparison. ① Olivine crystallization and accumulation at depth from a mantle-derived picritic magma (M_0); ② contamination of the fractionated magma (M_1) with the lower crust and sulfide segregation, ③ the Jinbaoshan deposit may have formed by early sulfide segregation; ④ formation of a daughter magma (M_2) that is depleted in PGE due to sulfide segregation; ⑤ formation of olivine cumulates from the daughter magma; ⑥ contamination of the daughter magma with the upper crust (M_3) and the 2nd stage sulfide segregation, ⑦ concentration of sulfides from the 2nd-stage segregation event to form the Limahe deposit. fc_1 — fraction of the lower crust contaminant; fc_2 — fraction of the upper crust contaminant. Inset is a general model which relates ore formation at Limahe to regional magmatism including basaltic volcanism. A_1 and A_2 — magma chamber in the lower crust, where the plume-derived melts experienced crustal contamination and sulfide segregation. B — magma chamber in the upper crust, where the daughter magma experienced another crustal contamination and sulfide segregation. LC — lower crust; UC — upper crust; SCLM — subcontinental lithospheric mantle; ECFB — Emeishan continental flood basalts; LMH — the Limahe deposit; JBS — the Jinbaoshan deposit. The γOs values for the SCLM, LC and UC are from Lambert et al. (1999).

6. Conclusions

(1) Variations of Re–Os isotopic compositions in the Limahe intrusion and associated sulfide ores are consistent with successive contamination of a mantle-derived magma with the lower and upper crusts at depth.
(2) The sulfide ores of the Limahe deposit have Re–Os concentrations and isotopic compositions that are similar to the immiscible sulfide liquids that may have segregated from a 2nd-stage magma that was depleted in PGE due to previous sulfide segregation.
(3) Significantly higher $\gamma Os_{(260\,Ma)}$ values in the sulfide ores than in the associated sulfide-barren websterites suggest that crustal contamination played a critical role in sulfide saturation during magma ascent.
(4) Significant differences in Re–Os isotopes between sulfide-bearing and sulfide-barren ultramafic rocks in the Limahe intrusion suggest that multiple pulses of magma with variable crustal contamination were involved in the formation of Limahe intrusion.

Acknowledgements

We thank Dr. Steve Barnes and an anonymous reviewer for their constructive reviews, and the guest editors of this special issue for their editorial inputs. This study was supported by the National 973

Program of China (2007CB411408), the Chinese Academy of Sciences (KZCX2-YW-Q04-06), the National Science Foundation of China (grants 40773033, 40730420, 40973039), the "Hundred Talents" Project from Chinese Academy of Sciences to Qi (KZCX2-YW-BR-09), and research fund from the State Key Laboratory of Ore Deposit Geochemistry of China (200905).

References

Ali, J.R., Thompson, G.M., Zhou, M.F., Song, X.Y., 2005. Emeishan large igneous province, SW China. Lithos 79, 475–489.
Arndt, N.T., Lesher, C.M., Czamanske, G.K., 2005. Mantle-derived magmas and magmatic Ni–Cu–(PGE) deposits. Economic Geology 100, 5–23.
Arndt, N.T., Czamanske, G., Walker, R.J., Chauvel, C., Fedorenko, V., 2003. Geochemistry and origin of the intrusive hosts of the Noril'sk-Talnakh Cu–Ni–PGE sulfide deposits. Economic Geology 98, 495–515.
Barnes, S.J., 2004. Komatiites and nickel sulfide ores of the Black Swan area, Yilgarn Craton, Western Australia. 4. Platinum group element distribution in the ores, and genetic implications. Miner. Deposita 39, 752–765.
Barnes, S.J., Lightfood, P.C., 2005. Formation of magmatic nickel sulfide ore deposits and processes affecting their copper and platinum group element contents. Economic Geology 100, 179–213.
Barnes, S.J., Zientek, M.L., Severson, M.J., 1997. Ni, Cu, Au and platinum-group element contents of sulphides associated with intraplate magmatism. Can. J. Earth Sci. 34, 337–351.
Brenan, J.M., 2008. Re–Os fractionation by sulfide melt–silicate melt partitioning: a new spin. Chem. Geol. 248, 140–165.
Campbell, I.H., Naldrett, A.J., 1979. The influence of silicate:sulfide ratios on the geochemistry of magmatic sulfides. Economic Geology 74, l503–l505.
Chung, S.L., Jahn, B.M., 1995. Plume–lithosphere interaction in generation of the Emeishan flood basalts at the Permian–Triassic boundary. Geology 23, 889–892.
Esser, B.K., Turekian, K.K., 1993. The osmium isotopic composition of the continental crust. Geochim. Cosmochim. Acta 57, 3093–3104.
Fan, W.M., Zhang, C.H., Wang, Y.J., Guo, F., Peng, T.P., 2008. Geochronology and geochemistry of Permian basalts in western Guangxi Province, Southwest China: evidence for plume–lithosphere interaction. Lithos 102, 218–236.
Fleet, M.E., Crocket, J.H., Liu, M., Stone, W.E., 1999. Laboratory partitioning of platinum group elements (PGE) and gold with application of magmatic sulfide–PGE deposits. Lithos 47, 127–142.
Hanski, E., Walker, R.J., Huhma, H., Polyakov, G.V., Balykin, P.A., Hoa, T.T., Phuong, N.T., 2004. Origin of the Permian–Triassic komatiites, northwestern Vietnam. Contrib. Mineral. Petrol. 147, 453–469.
He, B., Xu, Y.G., Chung, S.L., Xiao, L., Wang, Y.M., 2003. Sedimentary evidence for a rapid, kilometer-scale crustal doming prior to the eruption of the Emeishan flood basalts. Earth Planet. Sci. Lett. 213, 391–405.
Horan, M.F., Walker, R.J., Fedorenko, V.A., Czamanske, G.K., 1995. Osmium and neodymium isotopic constraints on the temporal and spatial evolution of Siberian flood basalt sources. Geochim. Cosmochim. Acta 59, 5159–5168.
Lambert, D.D., Foster, J.G., Frick, L.R., Li, C., Naldrett, A.J., 1999. Re–Os isotopic systematics of the Voisey's Bay Ni–Cu–Co magmatic ore system, Labrador, Canada. Lithos 47, 67–88.
Li, C., Ripley, E.M., Naldrett, A.J., 2003. Compositional variations of olivine and sulfur isotopes in the Noril'sk and Talnakh intrusions: implications for ore forming processes in dynamic magma conduits. Economic Geology 98, 69–86.
Li, C., Ripley, E.M., Naldrett, A.J., 2009. A new genetic model for the giant Ni–Cu–PGE sulfide deposits associated with the Siberian flood basalts. Economic Geology 104, 291–301.
Li, C., Maier, W.D., de Waal, S.A., 2001. Magmatic Ni–Cu versus PGE deposits: contrasting genetic controls and exploration implication. S. Afr. J. Geol. 104, 205–214.
Lightfoot, P.C., Keays, R.R., 2005. Siderophile and chalcophile metal variations in flood blasts from the Siberian trap, Noril'sk region: implications for the origin of the Ni–Cu–PGE sulfide ores. Economic Geology 100, 439–462.
Ma, Y.S., Tao, Y., Zhong, H., Zhu, F.L., Wang, X.Z., 2009. Geochemical constraints on the petrogenesis of the Abulangdang ultramafic intrusion, Sichuan Province. China. Acta Petrologica Sinica 25, 1146–1158 (in Chinese with English abstract).
Maier, W.D., Barnes, S.J., 2009. Formation of PGE deposits in layered intrusions. In: Li, C., Ripley, E.M. (Eds.), New Developments in Magmatic Ni–Cu and PGE Deposits. Geological Publishing House, Beijing, China, pp. 250–276.
Naldrett, A.J., 2009. Fundamenttals of magmatic sulfide deposits. In: Li, C., Ripley, E.M. (Eds.), New Developments in Magmatic Ni–Cu and PGE Deposits. Geological Publishing House, Beijing, China, pp. 1–26.
Naldrett, A.J., Li, C., 2009. Ore deposite related to flood basalts, Siberia. In: Li, C., Ripley, E. M. (Eds.), New Developments in Magmatic Ni–Cu and PGE Deposits. Geological Publishing House, Beijing, China, pp. 141–179.
Naldrett, A.J., Li, C., Ripley, E.M., 2009. Anorthosite-related Ni–Cu–Co deposits: examples from Labrador, Canada. In: Li, C., Ripley, E.M. (Eds.), New Developments in Magmatic Ni–Cu and PGE Deposits. Geological Publishing House, Beijing, China, pp. 192–218.
Pang, K.N., Li, C., Zhou, M.-F., Ripley, E.M., 2009. Mineral compositional constraints on petrogenesis and oxide ore genesis of the late Permian Panzhihua layered gabbroic intrusion, SW China. Lithos 110, 199–214.
Pang, K.N., Li, C., Zhou, M.F., Ripley, E.M., 2008. Abundant Fe–Ti oxide inclusions in olivine from the Panzhihua and Hongge layered intrusions, SW China: evidence for early saturation of Fe–Ti oxides in ferrobasaltic magma. Contrib. Mineral. Petrol. 156, 307–321.
Peach, C.L., Mathez, E.A., 1996. Constraints on the formation of platinum-group element deposits in igneous rocks. Economic Geology 91, 439–450.
Qi, L., Zhou, M.F., 2008. Platinum-group elemental and Sr–Nd–Os isotopic geochemistry of Permian Emeishan flood basalts in Guizhou Province, SW China. Chem. Geol. 248, 83–103.
Righter, K., Campbell, A.J., Humyun, M., Hervig, R.L., 2004. Partitioning of Ru, Rh, Pd, Re, Ir, and Au between Cr-bearing spinel, olivine, pyroxene and silicate melts. Geochim. Cosmochim. Acta 68, 867–880.
Ripley, E.M., Lambert, D.D., Frick, L.R., 1999. Re–Os, Sm–Nd, and Pb isotopic constraints on mantle and crustal contributions to magmatic sulfide mineralization in the Duluth Complex. Geochim. Cosmochim. Acta 62, 3349–3365.
Ripley, E.M., Shafer, P., Li, C., Hauck, S.A., 2008. Re–Os and O isotopic variations in magnetite from the contact zone of the Duluth Complex and the Biwabik Iron Formation, northeastern Minnesota. Chem. Geol. 249, 213–226.
Saal, A.E., Rudnick, R.L., Ravizza, G.E., Hart, S.R., 1998. Re–Os isotope evidence for the composition, formation and age of the lower continental crust. Nature 393, 58–61.
Shellnutt, J.G., Zhou, M.F., 2007. Permian peralkaline, peraluminous and metaluminous A-type granites in the Panxi district, SW China: their relationship to the Emeishan mantle plume. Chem. Geol. 243, 286–316.
Shellnutt, J.G., Wang, C.Y., Zhou, M.F., Yang, Y., 2009a. Zircon Lu–Hf isotopic compositions of metaluminous and peralkaline A-type granitic plutons of the Emeishan large igneous province (SW China): constraints on the mantle source. J. Asian Earth Sci. 35, 45–55.
Shellnutt, J.G., Zhou, M.F., Zellmer, G.F., 2009b. The role of Fe–Ti oxide crystallization in the formation of A-type granitoids with implications for the Daly gap: an example from the Permian Baima igneous complex, SW China. Chem. Geol. 259, 204–217.
Shirey, S.B., 1997. Re–Os isotopic composition of Mid-continent Rift System picrites and tholeiites: implications for plume lithosphere interaction and enriched mantle sources. Can. J. Earth Sci. 34, 489–503.
Smoliar, M.I., Walker, R.J., Morgan, J.W., 1996. Re–Os ages of group IIA, IIIA, IVA, and IVB iron meteorites. Science 271, 1099–1102.
Song, X.Y., Zhou, M.F., Hou, Z.Q., Cao, Z.M., Wang, Y.L., Li, Y.G., 2001. Geochemical constraints on the mantle source of the Upper Permian Emeishan continental flood basalts, southwestern China. International Geology Review 43, 213–225.
Song, X.Y., Zhou, M.F., Cao, Z.M., Sun, M., Wang, Y.L., 2003. Ni–Cu–(PGE) magmatic sulfide deposits in the Yangliuping area, Permian Emeishan igneous province, SW China. Miner. Deposita 38, 831–843.
Song, X.Y., Zhou, M.F., Tao, Y., Xiao, J.F., 2008. Controls on the metal compositions of magmatic sulfide deposits in the Emeishan large igneous province, SW China. Chem. Geol. 253, 38–49.
Song, X.Y., Keays, R.R., Zhou, M.F., Qi, L., Ihlenfeld, C., Xiao, J.F., 2009. Siderophile and chalcophile elemental constraints on the origin of the Jinchuan Ni–Cu–(PGE) sulfide deposit, NW China. Geochim. Cosmochim. Acta 73, 404–424.
Su, S.G., Li, C., Zhou, M.F., Ripley, E.M., Qi, L., 2008. Controls on variations of platinum-group element concentrations in the sulfide ores of the Jinchuan Ni–Cu deposit, western China. Miner. Deposita 43, 609–622.
Sun, X.M., Wang, S.W., Sun, W.D., Shi, G.Y., Sun, Y.L., Xiong, D.X., Qu, W.J., Du, A.D., 2008. PGE geochemistry and Re–Os dating of massive sulfide ores from the Baimazhai Cu–Ni deposit, Yunnan province, China. Lithos 105, 12–24.
Tang, Z.L., Song, X.Y., Su, S.G., 2009. Ni–Cu deposits related to high-Mg basaltic magma, Jinchuan, Western China. In: Li, C., Ripley, E.M. (Eds.), New Developments in Magmatic Ni–Cu and PGE Deposits. Geological Publishing House, Beijing, China, pp. 121–140.
Tao, Y., Li, C., Hu, R.Z., Ripley, E.M., Du, A.D., Zhong, H., 2007. Petrogenesis of the Pt–Pd mineralized Jinbaoshan ultramafic intrusion in the Permian Emeishan Large Igneous Province, SW China. Contrib. Mineral. Petrol. 153, 321–337.
Tao, Y., Li, C., Song, X.Y., Ripley, E.M., 2008. Mineralogical, petrological, and geochemical studies of the Limahe mafic–ultramatic intrusion and associated Ni–Cu sulfide ores, SW China. Miner. Deposita 43, 849–872.
Tao, Y., Ma, Y.S., Miao, L.C., Zhu, F.L., 2009. SHRIMP U–Pb zircon age of the Jinbaoshan ultramafic intrusion, Yunnan Province, SW China. Chinese Science Bulletin 54, 168–172.
Walker, R.J., Morgan, J.W., 1989. Rhenium–osmium systematics of carbonaceous chondrites. Science 243, 19–522.
Wang, C.Y., Zhou, M.F., Keays, R.R., 2006. Geochemical constraints on the origin of the Permian Baimazhai maficultramafic intrusion, SW China. Contrib. Mineral. Petrol. 152, 309–321.
Wang, C.Y., Zhou, M.-F., Qi, L., 2007. Permian flood basalts and mafic intrusions in the Jinping (SW China)–Song Da (northern Vietnam) district: mantle sources, crustal contamination and sulfide segregation. Chem. Geol. 243, 317–343.
Wang, C.Y., Zhou, M.F., Zhao, D., 2005. Mineral chemistry of chromite from the Permian Jinbaoshan Pt–Pd-sulphide-bearing ultramafic intrusion in SW China, with petrogenetic implications. Lithos 83, 47–66.
Xiao, L., Xu, Y.G., Mei, H.J., Zheng, Y.F., He, B., Pirajno, F., 2004. Distinct mantle sources of low-Ti and high-Ti basalts from the western Emeishan large igneous province, SW China: implications for plume–lithosphere interaction. Earth Planet. Sci. Lett. 228, 525–546.
Xu, J.F., Suzuki, K., Xu, Y.G., Mei, H.J., Li, J., 2007. Os, Pb, and Nd isotope geochemistry of the Permian Emeishan continental flood basalts: insights into the source of a large igneous province. Geochim. Cosmochim. Acta 71, 2104–2119.
Xu, Y.G., Chung, S.L., Jahn, B.M., Wu, G.Y., 2001. Petrological and geochemical constraints on the petrogenesis of the Permo-Triassic Emeishan flood basalts in southwestern China. Lithos 58, 145–168.
Xu, Y.G., He, B., Chung, S.L., Menzies, M.A., Frey, F.A., 2004. Geologic, geochemical, and geophysical consequences of plume involvement in the Emeishan flood-basalt province. Geology 32, 917–920.

Xu, Y.G., Luo, Z.Y., Huang, X.L., He, B., Xie, L.W., Shi, Y.R., 2008. Zircon U–Pb and Hf isotope constraints on crustal melting associated with the Emeishan mantle plume. Geochim. Cosmochim. Acta 72, 3084–3104.

Zhang, M., Reilly, S.Y.O., Wang, K.L., Hronsky, J., Griffin, W.L., 2008a. Flood basalts and metallogeny: The lithospheric mantle connection. Earth-Science Reviews 86, 145–174.

Zhang, Z.C., Mahoney, J.J., Mao, J.W., Wang, F.S., 2006. Geochemistry of picritic and associated basalt flows of the western Emeishan flood basalt province, China. Journal of Petrology 47, 1997–2019.

Zhang, Z.C., Mao, J.W., Mahoney, J.J., Wang, F.S., Qu, W.J., 2005. Platinum group elements in the Emeishan large igneous province, SW China: Implications for mantle sources. Geochemical Journal 39, 371–382.

Zhang, Z.C., Mao, J.W., Saunders, A.D., Ai, Y., Li, Y., Zhao, L., 2009. Petrogenetic modeling of three mafic–ultramafic layered intrusions in the Emeishan large igneous province, SW China, based on isotopic and bulk chemical constraints. Lithos 113, 369–392.

Zhang, Z.C., Zhi, X.C., Chen, L., Saunders, A.D., Reichow, M.K., 2008b. Re–Os isotopic compositions of picrites from the Emeishan flood basalt province, China. Earth Planet. Sci. Lett. 276, 30–39.

Zhong, H., Yao, Y., Prevec, S.A., Wilson, A.H., Viljoen, M.J., Viljoen, R.P., Liu, B.-G., Luo, Y.-N., 2004. Trace-element and Sr–Nd iso-topic geochemistry of the PGE-bearing Xinjie layered intrusion in SW China. Chem. Geol. 203, 237–252.

Zhong, H., Zhu, W.G., 2006. Geochronology of layered mafic intrusions from the Pan-Xi area in the Emeishan large igneous province, SW China. Miner. Deposita 41, 599–606.

Zhong, H., Zhu, W.G., Chu, Z.Y., He, D.F., Song, X.Y., 2007. SHRIMP U–Pb zircon geochronology, geochemistry, and Nd–Sr isotopic study of contrasting granites in the Emeishan large igneous province, SW China. Chem. Geol. 236, 112–133.

Zhong, H., Zhu, W.G., Qi, L., 2006. Platinum-group element (PGE) geochemistry of the Emeishan basalts in the Pan-Xi area, SW China. Chinese Science Bulletin 51, 845–854.

Zhou, M.F., Arndt, N.T., Malpas, J., Wang, C.Y., Kennedy, A.K., 2008. Two magma series and associated ore deposit types in the Permian Emeishan large igneous province, SW China. Lithos 103, 352–368.

Zhou, M.F., Malpas, J., Song, X.Y., Robinson, P.T., Sun, M., Kennedy, A.K., Lesher, C.M., Keays, R.R., 2002. A temporal link between the Emeishan large igneous province (SW China) and the end-Guadalu- pian mass extinction. Earth Planet. Sci. Lett. 196, 113–122.

Zhou, M.F., Robinson, P.T., Lesher, C.M., Keays, R.R., Zhang, C.J., Malpas, J., 2005. Geochemistry, petrogenesis, and metallogenesis of the Panzhihua gabbroic layered intrusion and associated Fe–Ti–V-oxide deposits, Sichuan Province, SW China. Journal of Petrology 46, 2253–2280.

Zhou, M.F., Zhao, J.H., Qi, L., Su, W., Hu, R.Z., 2006. Zircon U–Pb geochronology and elemental and Sr–Nd isotopic geochemistry of Permian mafic rocks in the Funing area, SW China. Contributions to Mineralogy and Petrology 151, 1–19.